Original Article

The effect of Nb on the microstructure and mechanical properties of wear-resistant steel heavy plates

Fábio Dian Murari [1*]
Adriana Marin Rodriguez Gusmão [2]
Leonardo de Oliveira Turani [3]

Abstract

The effect of Nb addition on the microstructure and mechanical properties of wear-resistant steel heavy plates processed by direct quenching was investigated on a pilot scale. The steels evaluated were laboratory-cast in a vacuum melting furnace, reheated to 1,250°C, and controlled rolled, aiming at the finishing step in the non-recrystallization region of austenite. The mechanical properties of the transformed microstructures were determined through hardness, tensile, and Charpy V-notch tests. The specimens were characterized using optical and scanning electron microscopy. An increase in strength and absorbed energy was observed with the increment of Nb content from 0.015 to 0.030%, demonstrating that this element was effective in refining the microstructure and making it more homogeneous, as confirmed by the microscopy analyses.

Keywords: Wear-resistant steels; Nb addition; Toughness; Heavy plates.

1 Introduction

Wear-resistant steels are characterized by having high surface hardness values, typically ranging from 300 to 600 HBW. They are mainly used in the form of heavy plates (thickness ranging from 8 to 72 mm) or hot-rolled strips [1].

As heavy plates, this type of material can be produced by direct quenching (DQ) after hot rolling or through an off-line quenching process. In the latter case, after conventional or controlled hot rolling followed by air cooling to room temperature, the plate is reaustenitized through conventional heating and subsequently quenched (RQ). In both cases, the microstructure is primarily composed of martensite with some degree of auto-tempering, characterized by the presence of transition carbides [2,3] and lower bainite [4]. Comparing the RQ and DQ processes, it is evident that the latter enables the production of heavy plates at significantly lower costs than those obtained via the RQ process, as the plates do not need to be reaustenitized after the rolling process.

Wear-resistant steels are also commonly designed to have high toughness [5]. Enhancing this property within a specific range not only improves abrasion resistance but also allows the material to be used in equipment subjected to high loading impacts and extremely cold environments, where a low ductile-to-brittle transition temperature is critical [6].

High-toughness wear-resistant steels can be obtained using a metallurgical strategy that results in excellent cleanliness, free from brittle inclusions and coarse precipitates, and with a fine and homogeneous austenitic grain size throughout the entire plate thickness [7].

As reported in the literature [8,9], the addition of Nb is essential for obtaining a refined and homogeneous microstructure and is used in steels processed by DQ and RQ. As mentioned by Pereda et al. [10], Nb delays the recrystallization of austenite by two mechanisms: (i) solute drag effect caused by the presence of solute atoms, and (ii) pinning effect due to strain-induced precipitates, the latter being the most effective. As a consequence, the austenite grains are work-hardened and elongated in the rolling direction during the finishing step, resulting in a pancake microstructure. If a high cooling rate is applied after rolling, a fine martensitic microstructure can be achieved, resulting in an improvement in the toughness of the final product [1].

Previous studies have shown that controlled rolling (CR) followed by DQ results in a superior balance of strength and toughness compared to conventional hot rolling processes [11,12]. However, this is only true for steels containing relatively large amounts of alloying elements, in which martensite formation occurs upon cooling despite the fine and heavily deformed austenite structure [1]. The high strength in these steels is attributed to the refined post-transformation microstructure and the inheritance of the austenite deformation substructure in the martensitic phase, i.e., the ausforming effect [13]. The improvement in toughness can also be attributed to the refinement of the martensitic structure [4,13]. Furthermore, it has been suggested that the superior toughness is related to a crystallographic texture developed in the austenite prior to

[1]Pesquisa e Desenvolvimento, Usinas Siderúrgicas de Minas Gerais - Usiminas, Ipatinga, MG, Brasil.
[2]Controle Integrado do Produto, Usinas Siderúrgicas de Minas Gerais - Usiminas, Ipatinga, MG, Brasil.
[3]Comercial, Usinas Siderúrgicas de Minas Gerais - Usiminas, Belo Horizonte, MG, Brasil.

[*]Corresponding author: fabio.murari@usiminas.com
Adresses: adriana.rodriguez@usiminas.com; leonardo.turani@usiminas.com

quenching, which can lead to delaminations or splitting in the Charpy specimens [11,14,15]. This has the beneficial effect of reducing the triaxial stress state at the crack tip and accordingly shifts the Charpy impact toughness transition temperature to lower values [16]. The other reason pointed out by Song et al. [4] is the greater lower bainite amount formed in DQ steels in comparison with RQ steels. In addition, the bainite in the RQ steels distributes along the prior austenite boundary fragmentarily, while in the DQ steels it extends into the prior austenite grains and segment them. This kind of bainite distribution decreases the martensite packet size as well as the block size, which may influence the mechanical properties to a large extent.

In this work, the effect of Nb content on the microstructure and mechanical properties of wear-resistant steel heavy plates processed by CR + DQ was investigated on a laboratory scale, aiming at achieving an optimum balance of toughness and strength, with absorbed energy values superior to 50 J in the rolling direction and 27 J in the transverse direction.

2 Material and methods

2.1 Material

The steels evaluated in this investigation were manufactured in a vacuum induction furnace and cast into ingots with an initial thickness of 135 mm. The chemical composition of these materials is shown in Table 1.

The Nb addition was carried out so that the carbonitrides rich in this element, of the type (Nb,Ti)(C,N), could be completely dissolved during the reheating of the ingots. As can be seen in Figure 1, obtained using the Thermo-Calc software, the temperatures for complete dissolution of this type of precipitate are 1103 °C for Nb15 steel and 1170 °C for the Nb30 steel. These values are within the slab reheating temperature limits usually practiced for microalloyed steels in current industrial rolling facilities (1100 to 1300 °C).

In order to minimize the formation of coarse Ti-rich carbonitrides, (Ti,Nb)(N,C), which are quite detrimental to toughness [8], the Ti, N, C and Nb contents were adjusted so that precipitation occurred after or towards the end of the solidification of the steels, as can be seen from Figure 1.

2.2 Hot rolling

The ingots were soaked at 1,250 °C for 30 min and controlled rolled in a pilot mill aiming at the finishing step in the non-recrystallization region of austenite, i.e. below the recrystallization stop temperature (RST) [7], which was calculated using the Boratto equation modified by Stalheim [17] for steels with C content of 0.12% or more, Equation 1 (chemical elements in wt.%). Both materials were subjected to the same per pass reduction schedule in order to obtain a final thickness of 21 mm, Figure 2. The total reduction applied below the RST was superior to 70% and some finishing passes were carried out with a reduction greater than 15%, as suggested by Stalheim [7]. The roughing stage, in contrast, was carried out with lighter passes, resulting in reductions of less than 10% due to the limitations of the pilot rolling mill. The total reduction employed in this step was equal to 45%.

$$\begin{gathered} RST = 887 + 464C + 6445\left(0.80.Nb\right) - 644\sqrt{\left(0.80.Nb\right)} + \\ 732\left(0.80.V\right) - 230\sqrt{\left(0.80.\mathrm{V}\right)} + 890\left(0.80.\mathrm{Ti}\right) + \\ 363\left(0.80.\mathrm{Al}\right) - 357\left(0.80.\mathrm{Si}\right) \end{gathered} \tag{1}$$

2.3 Microstructural characterization

Longitudinal sections of the rolled plates were prepared following standard metallographic procedures and examined by optical microscopy (ZEISS Imager.A1m) and field emission gun scanning electron microscopy (FEG-SEM, CARL ZEISS ULTRA 55 PLUS).

2.4 Mechanical properties

The hardness was measured on a FV-100 Vickers hardness tester according to ASTM E384:2022 [18] applying test force of 10 kgf. Tensile specimens with 25 mm gauge length longitudinal (L) and transverse (T) to rolling direction were machined for evaluation of the yield strength (YS), tensile strength (TS) and total elongation (TE). The tests were carried out in an electromechanical INSTRON 5882 machine according to ASTM A370:2023 [19], at a constant strain rate of $10^{-3}s^{-1}$. Impact toughness was measured with Charpy-V impact testing machine (RKP450 model) at 0, -20, -40 and -60 °C using longitudinal and transverse full-size specimens in agreement with ASTM A370:2023 [19].

3 Results and discussion

3.1 Prior austenite

Figure 3 shows the prior austenite grain size (PAGS) of the steels evaluated. The Nb15 steel exhibited an austenitic

Table 1. Chemical composition of the microalloyed steels used in this study (wt.%)

Steel	C	Mn	Si	Nb	Cr	Ti	N
Nb15	≤ 0.25	≤ 1.50	≤ 0.50	0.016	≤ 1.5	≤ 0.02	≤ 0.0050
Nb30				0.030			

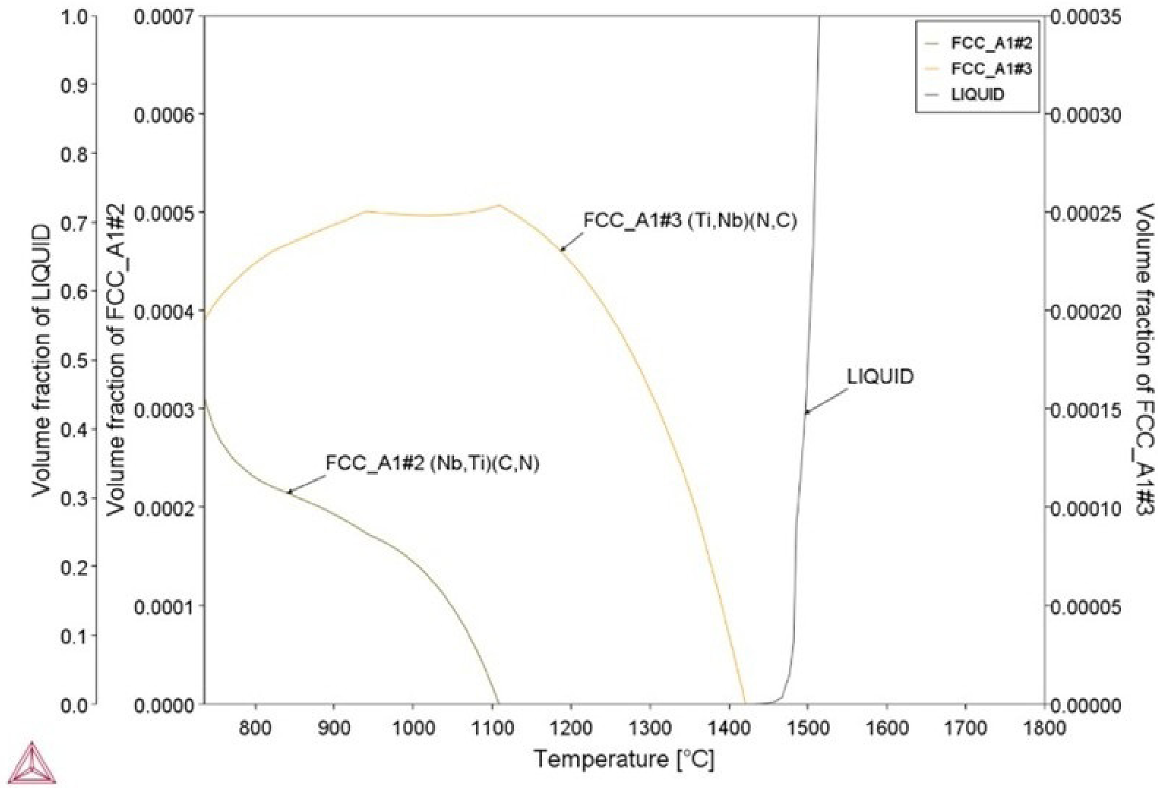

Figure 1(a).

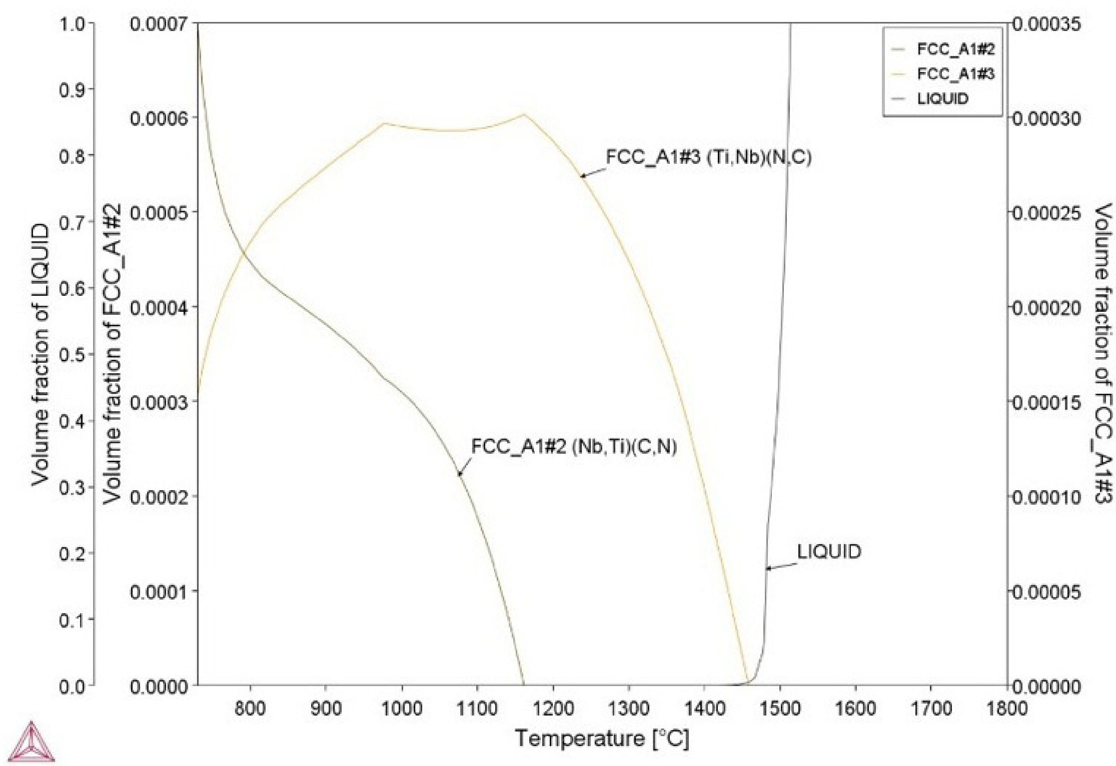

Figure 1(b).

Figure 1. Molar fraction of precipitates and liquid as a function of temperature, determined by Thermo-Calc software (Thermo-Calc for Windows, version 2024a and TCFE9 database).

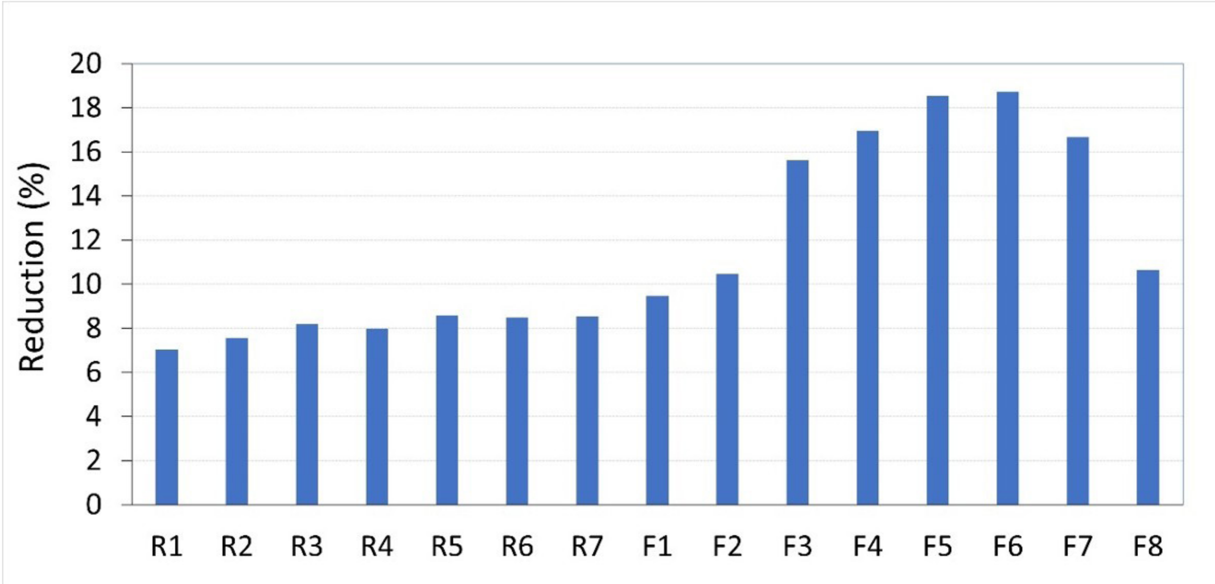

Figure 2. Per pass reduction schedule used during pilot rolling. R: roughing pass. F: Finishing pass.

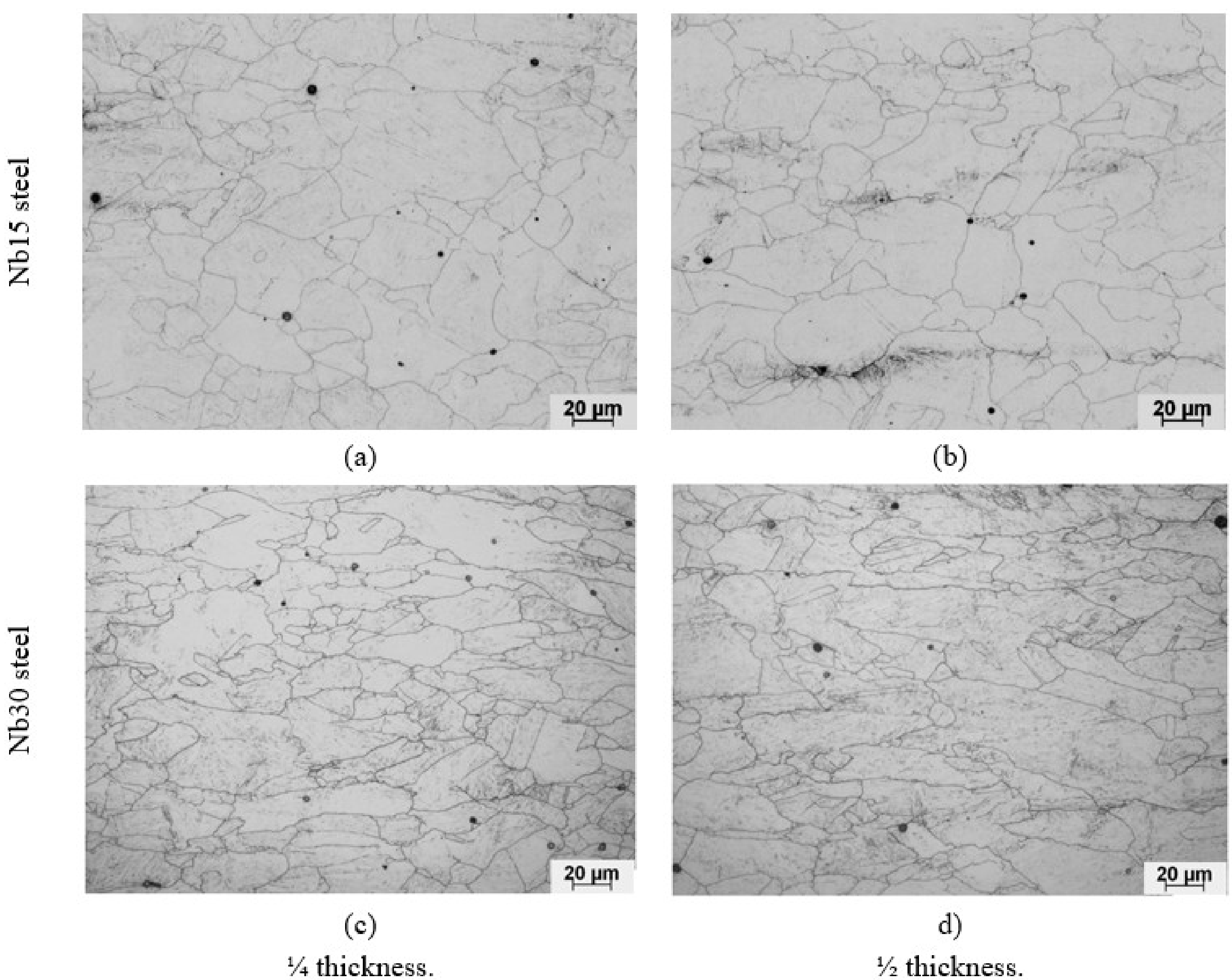

Figure 3. PAGS aspect of the steels studied after pilot rolling observed via optical microscopy.

grain distribution without evident pancaking, which can be attributed to the lower reduction in the non-recrystallization region of austenite. With the increase in Nb content in Nb30 steel, a more pronounced pancaking of the austenitic grains is observed, which is due to an increase in RST. However, significant heterogeneity is still present, which may be associated with the execution of the last roughing passes and/or the first finishing passes in the partial recrystallization region, between recrystallization limit temperature (RLT) and RST [7,17].

3.2 Final microstructure

As shown in Figure 4, the alloys studied exhibited a predominantly martensitic microstructure with some degree of auto-tempering, as evidenced by the presence of carbides within the laths (indicated by white arrows), a characteristic feature of this type of steel [2,3]. Additionally, as mentioned earlier, some amount of lower bainite appears to have formed.

3.3 Effect of Nb on the mechanical properties

As shown in Figure 5, the Nb content had no significant influence on the Vickers hardness of the evaluated alloys, with average values of 435 and 436 HV10 obtained along the thickness for the Nb15 and Nb30 steels, respectively.

It is worth noting that the hardness values of the analyzed alloys presented a very homogeneous profile throughout the thickness, with no evidence of significant chemical segregation in the center of the thickness.

As shown in Figure 6, the increase in Nb content led to a slight increase in YS and TS. Additionally, there was an improvement in ductility, as indicated by the TE. The increase in mechanical resistance with the increment of Nb content can be associated mainly with the refinement of the microstructure and the greater accumulated strain during hot rolling. Furthermore, a greater amount of lower bainite may have been formed in the Nb30 steel.

As mentioned earlier, the lower bainite in the DQ steels extends into the prior austenite grains, segmenting them. This type of bainite distribution decreases both the martensite packet size and the block size, which may influence the mechanical properties. However, this issue requires further investigation.

It is also possible to note in Figure 6 that transverse specimens presented higher YS and TS. This phenomenon was also observed by Weiss and Thompson [11] and Kaijalainen et al. [15] in direct-quenched and tempered steels,

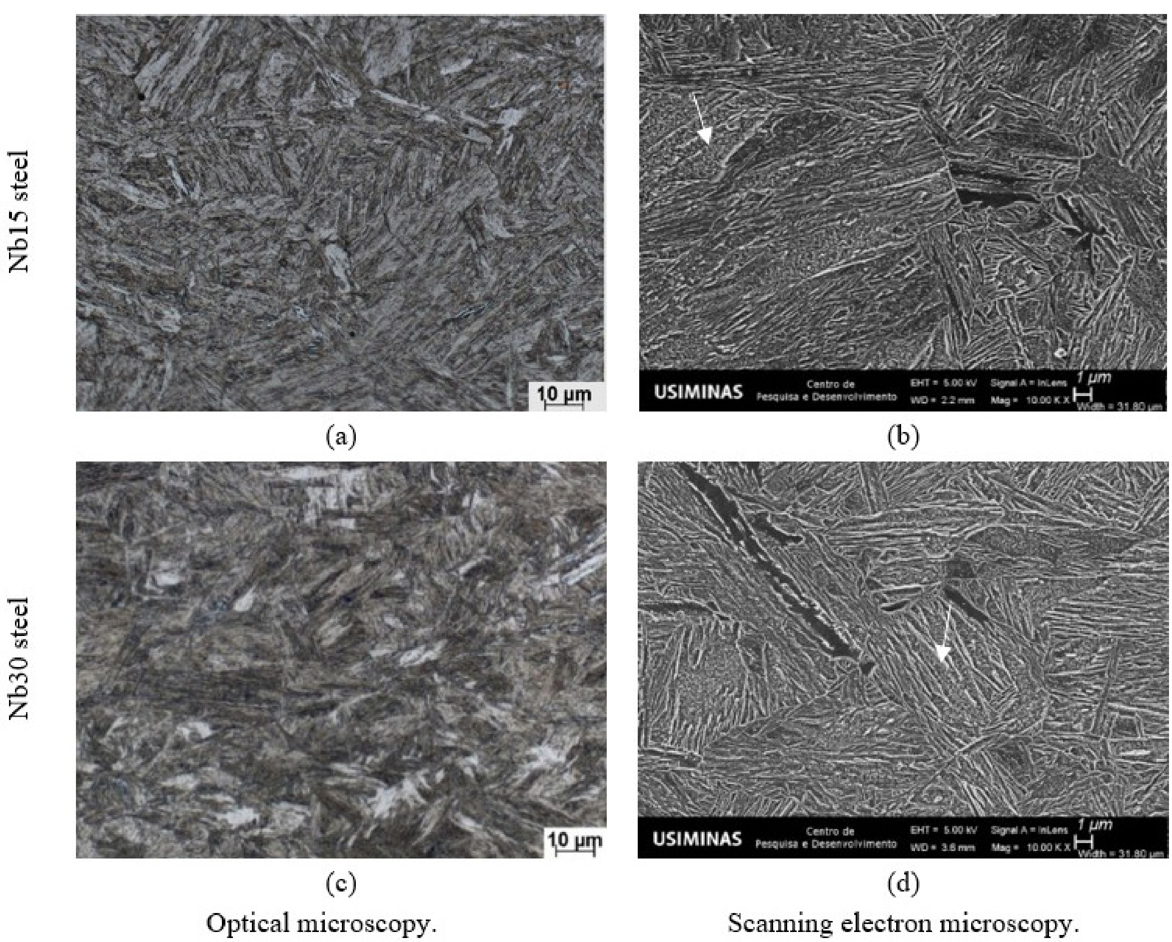

Figure 4. Final microstructure of the steels evaluated. ¼ of the thickness. Etching: Nital 4% (optical microscopy) and 2% (scanning electron microscopy).

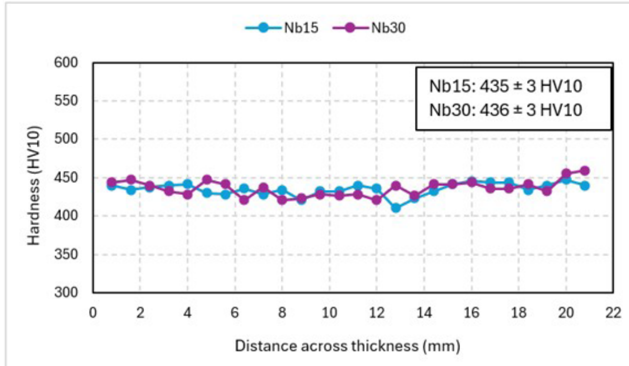

Figure 5. Vickers hardness profile along the thickness of the studied steels.

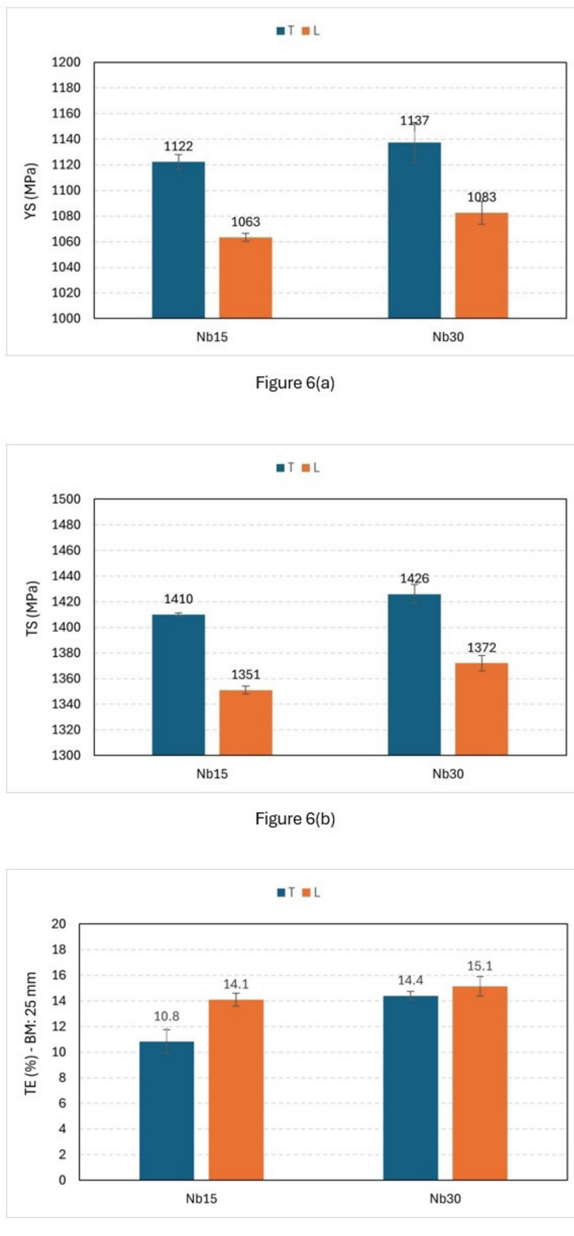

Figure 6. Variation of yield strength (a), tensile strength (b), and total elongation (c) with Nb content.

and may be related to specimen texture effects. Concerning TE, it can be seen that the higher values were obtained for longitudinal specimens, which is also in agreement with the authors mentioned above. However, the increase in the Nb content slightly reduced the difference between the longitudinal and transverse directions.

3.4 Effect of Nb on the toughness

The effect of increasing Nb content on the absorbed energy can be observed in Figure 7.

According to the presented data, the alloys evaluated resulted in absorbed energy values exceeding 50 J at -40 °C in the longitudinal direction and 27 J at -20 °C in the transverse direction, meeting current customer requirements for this type of material and aligning with the objectives of this study. Furthermore, it is worth noting that the energy values in the longitudinal direction remain above 50 J at -60 °C, which is a very significant result for a wear-resistant martensitic steel processed by DQ.

Concerning the Nb influence, it is possible to note that the increase in its content, from 0.015 to 0.030%, contributed to the improvement of toughness, in addition to promoting an increase in mechanical resistance. This suggests that Nb was effective in refining and homogenizing the microstructure, as indicated by the microstructural analyses (PAGS aspect) and by the lower variability in the Charpy V-notch tests.

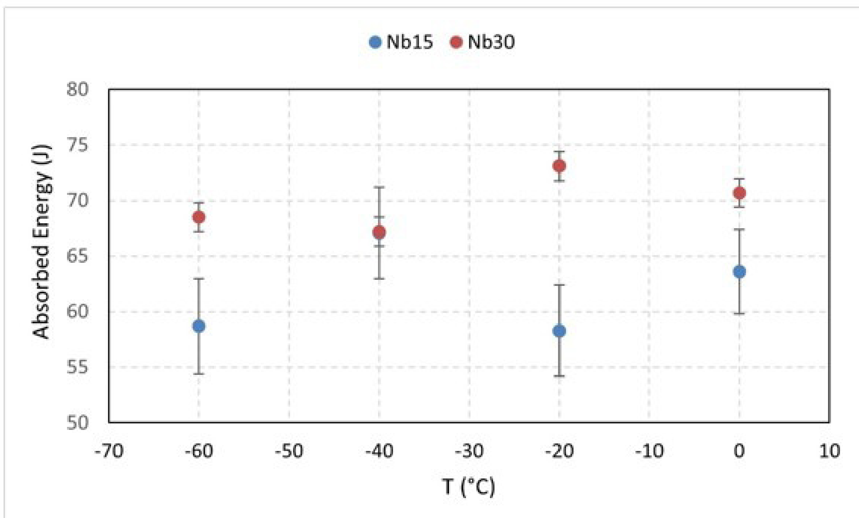

(a) Longitudinal direction.

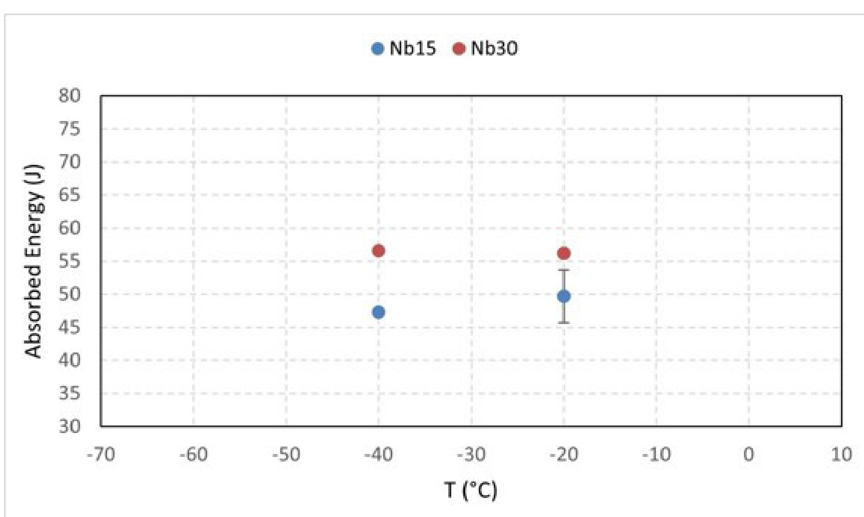

(b) Transverse direction.

Figure 7. Absorbed energy values for the alloys studied. Four specimens were tested for each temperature.

4 Conclusions

The investigated wear-resistant steels exhibited absorbed energy values above 50 J at -40 °C in the longitudinal direction and 40 J at -20 °C in the transverse direction, results that are quite satisfactory for this type of material, with a hardness superior to 430 HV10.

The increase in Nb content, from 0.015 to 0.030%, contributed to improving toughness, resulting in absorbed energy values greater than 65 J between 0 and -60 °C, in addition to promoting an increase in the mechanical resistance of the wear-resistant steel studied, which is an evidence that this element was effective in refining the microstructure and making it more homogeneous.

The results obtained indicate that carrying out the finishing step in the non-recrystallization region of austenite, with a total reduction above 70%, is an effective strategy for obtaining martensitic steels with excellent toughness. Furthermore, they suggest that performing the finishing stage under these conditions can compensate, to a certain extent, the accomplishment of the roughing stage, particularly the last passes, in the region of partial recrystallization of austenite. However, the influence of processing conditions at the roughing stage for the steel evaluated is a subject that requires further investigation.

References

1 Schneider AS, Cayla JL, Just C, Schwinn V. The role of niobium for the development of wear resistant steels with superior toughness. In: International Symposium on Wear Resistant Alloys for the Mining and Processing Industry; 2015 May 4-7; Campinas, Brazil. USA: TMS; 2015. p. 173-186.

2 Gutman L. Selection of high-temperature abrasion resistant steels for the mining and processing industry. Materials Engineering [master's]. Norrbotten: Department of Engineering Sciences and Mathematics, Lulea University of Technology; 2020. 39 p.

3 Deng XT, Fu TL, Wang ZD, Misra RDK, Wang GD. Epsilon carbide precipitation and wear behavior of low alloy wear resistant steels. Materials Science and Technology. 2016;32(4):320-327.

4 Song H, Zhang S, Lan L, Li C, Liu H, Zhao D, et al. Effect of direct quenching on the microstructure and mechanical properties of a wear-resistant steel. Acta Metallurgica. 2013;26(4):390-398.

5 Zou JL, Liu SL, Zheng ZB, Long J, Huang Y, Zheng KH, et al. Research on impact-abrasion-corrosion behavior of three typical wear-resistant steels under high impact energy. Journal of Materials Engineering and Performance. 2022;31(6):4343-4353.

6 Mohrbacher H, Morris JW, Krauss G. Fundamentals and practical approaches of optimizing martensitic steels for use under severe operating conditions. In: International Symposium on Wear Resistant Alloys for the Mining and Processing Industry; 2015 May 4-7; Campinas, Brazil. USA: TMS; 2015. p. 93-158.

7 Stalheim D. Metallurgical strategy for optimized production of QT high-strength and abrasion-resistant plate steels. Pittsburgh, USA: AISTech; 2019. p. 1881-1892.

8 Murari FD, Santos AA, Costa e Silva ALV, Rodriguez-Ibabe JM. The effect of reheating temperature on the dissolution of precipitates and mechanical Properties of microalloyed steel heavy plates. In: Proceedings of the 11th International Rolling Conference - IRC 2019; 56th Rolling and Metal Forming Seminar; 2019; São Paulo, Brazil. São Paulo: ABM; 2019. 12 p.

9 Sanz L, Pereda B, López B. Effect of thermomechanical treatment and coiling temperature on the strengthening mechanisms of low carbon steels microallowed with Nb. Materials Science and Engineering A. 2017;685:377-390.

10 Pereda B, Rodriguez-Ibabe JM, López B. Improved model of kinetics of strain induced precipitation and microstructure evolution of Nb microalloyed steels during multipass rolling. ISIJ International. 2008;48(10):1457-1466.

11 Weiss RK, Thompson SW. Strength differences between direct-quenched and reheated-and-quenched plate steels. In: Thompson SW, Taylor KA, Fletcher FB, editors. Physical metallurgy of direct-quenched steels, USA: TMS; 1993, pp. 107-38.

12 Muckelroy NC, Findley KO, Bodnar RL. Microstructure and mechanical properties of direct quenched versus conventional reaustenitized and quenched plate. Journal of Materials Engineering and Performance. 2013;22: 512-522.

13 Okamoto K, Yoshie A, Nakao H. Physical metallurgy of direct-quenched steel plates and its application for commercial processes and Products. In: Thompson SW, Taylor KA, Fletcher FB, editors. Physical metallurgy of direct-quenched steels. USA: TMS; 1993. p. 339-405.

14 Taylor KA, Hansen SS. Effects of vanadium and processing parameters on the structure and properties of a direct-quenched low-carbon Mo-B steel. Metallurgical Transactions A, 22, 1991, pp. 2.359-2.374.

15 Kaijalainen AJ, Suikkanen PP, Karjalainen LP, Kömi JI, DeArdo AJ. Effect of austenite conditioning in the non-recrystallization regime on the microstructure and Properties of ultra high strength strip steel with bainitic/martensitic microstructures. In: Proceedings of the 2nd International Conference on Super-High Strength Steels; 2010; Peschiera del Garda, Italy. Milano: Associazione Italiana di Metallurgia -AIM; 2010.

16 Bramfitt BL, Marder AR. A study of the delamination behaviour of a very low-carbon steel. Metallurgical Transactions *A*, 1997:8:1263-1273.

17 Stalheim DG. Recrystallization behaviors in the production of structural steels. In: Technical contribution to the 52º Rolling Seminar – Processes and Rolled & Coated Products, part of the ABM Week, 2015 August 17-21; Rio de Janeiro, Brazil. São Paulo: ABM; 2015.

18 American Society for Testing and Materials. ASTM E-384: 2022; Test Method for Microindentation Hardness of Materials. Philadelphia: ASTM; 2022.

19 American Society for Testing and Materials. ASTM A-370: 2023; Test Methods and Definitions for Mechanical Testing of Steel Products. Philadelphia: ASTM; 2023.

Received: 1 Oct. 2025
Accepted: 16 Oct. 2025

Editor-in-charge:
André Luiz Vasconcellos da Costa e Silva